

# I'm Me, We're Us, and I'm Us: Tri-directional Contrastive Learning on Hypergraphs

Dongjin Lee<sup>1</sup> and Kijung Shin<sup>1,2</sup>

<sup>1</sup>School of Electrical Engineering, KAIST, South Korea

<sup>2</sup>Kim Jaechul Graduate School of AI, KAIST, South Korea  
 {dongjin.lee, kijungs}@kaist.ac.kr

## Abstract

Although machine learning on hypergraphs has attracted considerable attention, most of the works have focused on (semi-)supervised learning, which may cause heavy labeling costs and poor generalization. Recently, contrastive learning has emerged as a successful unsupervised representation learning method. Despite the prosperous development of contrastive learning in other domains, contrastive learning on hypergraphs remains little explored. In this paper, we propose **TriCon** (Tri-directional Contrastive learning), a general framework for contrastive learning on hypergraphs. Its main idea is tri-directional contrast, and specifically, it aims to maximize in two augmented views the agreement (a) between the same node, (b) between the same group of nodes, and (c) between each group and its members. Together with simple but surprisingly effective data augmentation and negative sampling schemes, these three forms of contrast enable TriCon to capture both microscopic and mesoscopic structural information in node embeddings. Our extensive experiments using 13 baseline approaches, five datasets, and two tasks demonstrate the effectiveness of TriCon, and most noticeably, TriCon consistently outperforms not just unsupervised competitors but also (semi-)supervised competitors mostly by significant margins for node classification.

## 1 Introduction

Many real-world interactions are group-wise. Examples include collaborations of researchers, discussions on online Q&A sites, group conversations on messaging apps, co-citations of documents, and co-purchases of items. A hypergraph is a suitable option to model such group-wise interactions [Benson et al., 2018, Do et al., 2020, Lee et al., 2020]. A *hypergraph*, which is a generalized graph, allows an edge to join an arbitrary number of nodes, and thus each such edge, which is called a *hyperedge*, naturally represents a group-wise interaction.

Recently, machine learning on hypergraphs has drawn a lot of attention from a broad range of fields, including social network analysis [Yang et al., 2019], recommender systems [Xia et al., 2021], and bioinformatics [Zheng et al., 2019]. Hypergraph-based approaches often outperform graph-based ones on various machine learning tasks, including classification [Feng et al., 2019], clustering [Benson et al., 2016], ranking [Yu et al., 2021], and outlier detection [Lee et al., 2022].

Previous studies have largely focused on developing encoder architectures so-called *hypergraph neural networks* for hypergraph-structured data [Feng et al., 2019, Yadati et al., 2019, Dong et al., 2020, Bai et al., 2021, Arya et al., 2020], and in most cases, such hypergraph neural networks are trained in a (semi-)supervised way. However, data labeling is often time, resource, and labor-intensive, and neural networks trained only in a supervised way can easily overfit and may fail to generalize [Rong et al., 2020], making it difficult to be applied to other tasks.

Thus, self-supervised learning [Liu et al., 2022, Jaiswal et al., 2020, Liu et al., 2021], which does not require labels, have become popular, and especially contrastive learning has achieved great success in computer vision [Chen et al., 2020, Hjelm et al., 2019] and natural language processing [Gao et al., 2021]. Contrastive learning has proved effective also for learning on (ordinary) graphs [Veličković et al., 2018a, Peng et al., 2020, Hassani and Khasahmadi, 2020, Zhu et al., 2020, 2021, You et al., 2020], and a common approach is to (a)

create two augmented views from the input graph and (b) learn machine learning models to maximize the agreement between the two views.

However, contrastive learning on hypergraphs remains largely underexplored with only a handful of previous studies [Xia et al., 2021, Zhang et al., 2021, Yu et al., 2021] (see Section 2 for details). Especially, the following questions remain open: (Q1) what to contrast in a hypergraph?, (Q2) how to augment a hypergraph?, and (Q3) how to select negative samples?

For Q1, which is our main focus, we propose *tri-directional contrast*. In addition to *node-level contrast*, which is the only form of contrast employed in the previous studies, we propose the use of *group-level* and *membership-level* contrast. That is, we aim to maximize in two augmented views to agreement (a) between the same node, (b) between the same group of nodes and (c) between each group and its members. These three forms of contrast are complementary, leading to representations that capture not just microscopic but also mesoscopic (i.e., higher-order) relations between nodes. In addition, for Q2, we demonstrate that combining two simple augmentation strategies (spec., membership corruption and feature corruption) is effective. For Q3, we reveal that uniform random sampling is surprisingly successful, and in our experiments, even an extremely small sample size leads to marginal performance degradation.

Our proposed method TriCon, which is based on the aforementioned observations, is evaluated extensively using 13 baseline approaches, five datasets, and two tasks. The most notable result is that, for node classification, TriCon outperforms not just unsupervised competitors but also all (semi-)supervised competitors on all considered datasets, mostly by considerable margins. Moreover, we demonstrate the consistent effectiveness of tri-directional contrast, which is our main contribution.

## 2 Related Work

**Hypergraph learning** Due to its enough expressiveness to capture higher-order structural information, learning on hypergraphs has received a lot of attention. Many recent studies have focused on generalizing graph neural networks (GNNs) to hypergraphs [Feng et al., 2019, Bai et al., 2021, Yadati et al., 2019]. Most of them redefine hypergraph message aggregation schemes based on clique expansion (i.e., replacing hyperedges with cliques to obtain a graph) or its variants. While its simplicity is appealing, clique expansion causes structural distortion and leads to undesired information loss [Hein et al., 2013, Li and Milenkovic, 2018]. On the other hand, HNHN [Dong et al., 2020] extends star expansion by using two different weight matrices for node- and hyperedge-side message aggregations. Arya et al. [2020] propose HyperSAGE for inductive learning on hypergraphs based on two-stage message aggregation. Several studies attempt to unify hypergraphs and GNNs [Huang and Yang, 2021, Zhang et al., 2022]; and Chien et al. [2022] generalize propagation methods of most existing hypergraph neural networks as a multiset function learned by Deep Sets [Zaheer et al., 2017] and Set Transformer [Lee et al., 2019]. Most approaches above use (semi-)supervised learning.

**Contrastive learning** In the computer vision domain, the latest contrastive learning frameworks (e.g., SimCLR [Chen et al., 2020] and MoCo [He et al., 2020]) leverage the changelessness of semantics under various image transformations, such as random flip, rotation, color distortion, etc, to learn visual features. They aim to learn distinguishable representations by contrasting positive and negative pairs.

In the graph domain, many traditional unsupervised representation learning methods follow the contrastive paradigm [Perozzi et al., 2014, Grover and Leskovec, 2016, Hamilton et al., 2017], considering nodes that appear in the same random walk as positive samples. However, these random-walk-based methods tend to overemphasize the structural information and disregard the attributes of entities. On the other hand, DGI [Veličković et al., 2018a] combines the power of GNNs and contrastive learning, which seeks to maximize the mutual information between node embeddings and graph embeddings. Recently, a number of graph contrastive learning approaches [You et al., 2020, Zhu et al., 2020, 2021, Hassani and Khasahmadi, 2020] that follow a common framework [Chen et al., 2020] have been proposed. Although these methods have achieved state-of-the-art performance on their task of interest, they cannot naturally exploit group-wise interactions, which we focus on in this paper.

**Hypergraph contrastive learning** Contrastive learning on hypergraphs is still in its infancy. Recently, several studies explore contrastive learning on hypergraphs in the context of recommendation [Zhang et al.,

2021, Xia et al., 2021, Yu et al., 2021]. For example, Zhang et al. [2021] proposes S<sup>2</sup>-HHGR for group recommendation, which applies contrastive learning to remedy a data sparsity issue. In particular, they propose a hypergraph augmentation scheme that uses a coarse- and fine-grained node dropout for each view. However, they do not consider group-wise contrast. Although Xia et al. [2021] employ group-wise contrast for session recommendation, they do not account for node-wise and node-group pair-wise relationships when constructing a contrastive loss.

### 3 Proposed Method: TriCon

In this section, we describe TriCon, our proposed framework for hypergraph contrastive learning. First, we introduce some preliminaries on hypergraphs and hypergraph neural networks, and then we elucidate the problem setting and details of the proposed method.

#### 3.1 Preliminaries

**Hypergraphs and notation.** A *hypergraph*, a set of hyperedges, is a natural extension of a graph, allowing the hyperedge to contain any number of nodes. Formally, let  $H = (V, E)$  be a hypergraph, where  $V = \{v_1, v_2, \dots, v_{|V|}\}$  is a set of nodes and  $E = \{e_1, e_2, \dots, e_{|E|}\}$  is a set of hyperedges, with each hyperedge is a non-empty subset of  $V$ . The node feature matrix is represented by  $\mathbf{X} \in \mathbb{R}^{|V| \times F}$ , where  $\mathbf{x}_v = \mathbf{X}[v, :]^T \in \mathbb{R}^F$  is the feature of node  $v$ . In general, a hypergraph can alternatively be represented by its *incidence matrix*  $\mathbf{H} \in \{0, 1\}^{|V| \times |E|}$ , with entries defined as  $h_{ve} = 1$  if  $v \in e$ , and  $h_{ve} = 0$  otherwise. In other words,  $h_{ve} = 1$  when node  $v$  and hyperedge  $e$  form a *membership*. Each hyperedge  $e \in E$  is assigned a positive weight  $w_e$ , and all the weights formulate a diagonal matrix  $\mathbf{W} \in \mathbb{R}^{|E| \times |E|}$ . We use the diagonal matrix  $\mathbf{D}_V$  to represent the degree of vertices, where its entries  $d_v = \sum_e w_e h_{ve}$ . Also we use the diagonal matrix  $\mathbf{D}_E$  to denote the degree of hyperedges, where its element  $\delta_e = \sum_v h_{ve}$  represents the number of nodes connected by the hyperedge  $e$ .

**Hypergraph neural networks.** Modern hypergraph neural networks [Feng et al., 2019, Yadati et al., 2019, Bai et al., 2021, Dong et al., 2020, Arya et al., 2020, Chien et al., 2022] follow a two-stage neighborhood aggregation strategy: node-to-hyperedge and hyperedge-to-node aggregation. They iteratively update the representation of a hyperedge by aggregating representations of its incident nodes and the representation of a node by aggregating representations of its incident hyperedges. Let  $\mathbf{P}^{(k)} \in \mathbb{R}^{|V| \times F'_k}$  and  $\mathbf{Q}^{(k)} \in \mathbb{R}^{|E| \times F''_k}$  be the node and hyperedge representations at the  $k$ -th layer, respectively. Formally, the  $k$ -th layer of a hypergraph neural network is

$$\mathbf{q}_e^{(k)} = f_{V \rightarrow E}^{(k)} \left( \mathbf{q}_e^{(k-1)}, \{\mathbf{p}_v^{(k-1)} : v \in e\} \right), \quad \mathbf{p}_v^{(k)} = f_{E \rightarrow V}^{(k)} \left( \mathbf{p}_v^{(k-1)}, \{\mathbf{q}_e^{(k)} : v \in e\} \right) \quad (1)$$

where  $\mathbf{p}_v^{(0)} = \mathbf{x}_v$ . The choice of aggregation rules,  $f_{V \rightarrow E}(\cdot)$  and  $f_{E \rightarrow V}(\cdot)$ , is critical, and a number of models have been proposed. In HGNN [Feng et al., 2019], for example, they choose  $f_{V \rightarrow E}$  and  $f_{E \rightarrow V}$  to be the weighted sum over inputs with normalization as:

$$\mathbf{q}_e^{(k)} = \sum_{v \in e} \frac{\mathbf{p}_v^{(k-1)}}{\sqrt{d_v}}, \quad \mathbf{p}_v^{(k)} = \sigma \left( \frac{1}{\sqrt{d_v}} \sum_{e: v \in e} \frac{w_e \mathbf{q}_e^{(k)} \Theta^{(k)}}{\delta_e} + \mathbf{b}^{(k)} \right), \quad (2)$$

where  $\Theta^{(k)}$  is a learnable weight matrix,  $\mathbf{b}^{(k)}$  is a bias, and  $\sigma$  denotes a non-linear activation function. Many other hypergraph neural networks can be represented similarly to (1).

#### 3.2 Problem Setting: Hypergraph-based Contrastive Learning

Our objective is to train a hypergraph encoder,  $f_\theta : \mathbb{R}^{|V| \times F} \times \mathbb{R}^{|V| \times |E|} \rightarrow \mathbb{R}^{|V| \times F'} \times \mathbb{R}^{|E| \times F''}$ , such that  $f_\theta(\mathbf{X}, \mathbf{H}) = (\mathbf{P}, \mathbf{Q})$  produces low-dimensional representations of nodes and hyperedges in a fully unsupervised manner, specifically a contrastive manner. These representations may then be utilized for downstream tasks, such as node classification and clustering.

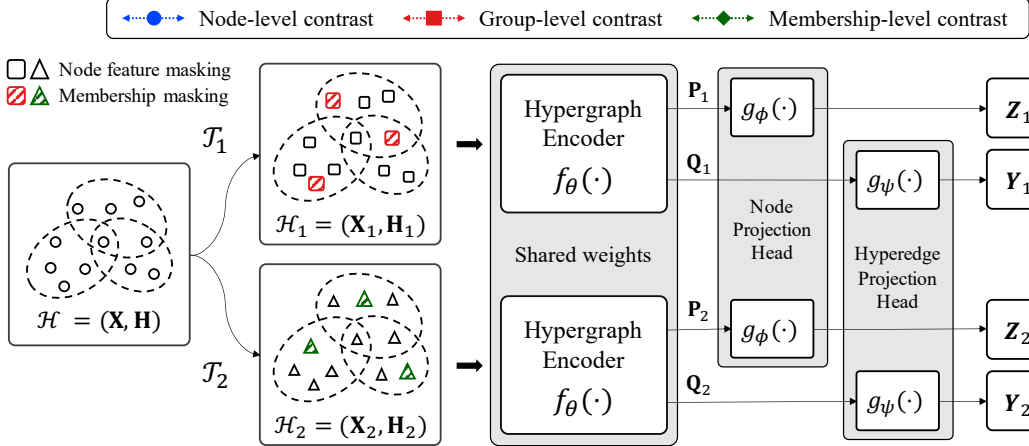


Figure 1: Overview of our proposed TriCon model. First, two different semantically similar views are generated by augmentations  $\mathcal{T}_1$  and  $\mathcal{T}_2$  from the original hypergraph. From these, we use a shared hypergraph encoder  $f_\theta(\cdot)$  to form node and hyperedge representations. After passing node and hyperedge representations to their respective projection heads (i.e.,  $g_\phi(\cdot)$  and  $g_\psi(\cdot)$ ), we maximize the agreement between two views via our proposed tri-directional contrast which is a combination of node-, group-, and membership-level contrast.

### 3.3 TriCon: Tri-directional Contrastive Learning

Basically, TriCon follows the conventional multi-view graph contrastive learning paradigm where the model tries to maximize the agreement of representations between different views [You et al., 2020, Hassani and Khasahmadi, 2020, Zhu et al., 2020]. While most existing approaches only used node-level contrast, the big difference between TriCon and these methods is that TriCon applies three forms of contrast for each of the three essential elements constituting hypergraphs: nodes, hyperedges, and node-hyperedge memberships. Figure 1 visually summarizes TriCon’s architecture. TriCon is composed of the following four major components:

**(1) Hypergraph augmentation.** We consider a hypergraph  $\mathcal{H} = (\mathbf{X}, \mathbf{H})$ . TriCon first generates two alternate views of the hypergraph  $\mathcal{H}$ :  $\mathcal{H}_1 = (\mathbf{X}_1, \mathbf{H}_1)$  and  $\mathcal{H}_2 = (\mathbf{X}_2, \mathbf{H}_2)$ , by applying stochastic hypergraph augmentation function  $\mathcal{T}_1$  and  $\mathcal{T}_2$  respectively. We use a combination of random *node feature masking* [You et al., 2020, Zhu et al., 2020] and *membership masking* to augment a hypergraph in terms of attributes and structure. Following previous studies [You et al., 2020, Thakoor et al., 2022], node feature masking is not applied to each node independently, and instead, we generate a single random binary mask of size  $F$  where each entry is sampled from a Bernoulli distribution  $\mathcal{B}(1 - p_f)$ , and use it to mask features of all nodes in the hypergraph. Similarly, we use a binary mask of size  $K = \text{nnz}(\mathbf{H})$  where each element is sampled from a Bernoulli distribution  $\mathcal{B}(1 - p_m)$  to mask node-hyperedge memberships. The degree of augmentation is controlled by  $p_f$  and  $p_m$ , and we can adopt different hyperparameters for each augmented view. More details and other types of hypergraph augmentation for contrastive learning are provided in Appendix D.

**(2) Hypergraph encoder.** A hypergraph neural network encoder  $f_\theta(\cdot)$  produces node and hyperedge representations,  $\mathbf{P}$  and  $\mathbf{Q}$  respectively, for two augmented views:  $(\mathbf{P}_1, \mathbf{Q}_1) := f_\theta(\mathbf{X}_1, \mathbf{H}_1)$  and  $(\mathbf{P}_2, \mathbf{Q}_2) := f_\theta(\mathbf{X}_2, \mathbf{H}_2)$ . TriCon does not constrain the choice of hypergraph encoder architectures if they can be formulated by (1). In our proposed method, we use a simple layer using the element-wise mean pooling as a special instance of (1). We choose  $f_{V \rightarrow E}$  and  $f_{E \rightarrow V}$  as:

$$\mathbf{q}_e^{(k)} = \sigma \left( \sum_{v \in e} \frac{\mathbf{p}_v^{(k-1)} \Theta_E^{(k)}}{\delta_e} + \mathbf{b}_E^{(k)} \right), \quad \mathbf{p}_v^{(k)} = \sigma \left( \sum_{e: v \in e} \frac{w_e \mathbf{q}_e^{(k)} \Theta_V^{(k)}}{d_v} + \mathbf{b}_V^{(k)} \right), \quad (3)$$

where  $\Theta_E^{(k)} \in \mathbb{R}^{F'_k \times F''_k}$  and  $\Theta_V^{(k)} \in \mathbb{R}^{F''_k \times F'_k}$  are trainable weights and  $\mathbf{b}_E^{(k)} \in \mathbb{R}^{F''_k}$  and  $\mathbf{b}_V^{(k)} \in \mathbb{R}^{F'_k}$  are biases. We use  $w_e = 1$  for simplicity, and (3) can be represented as (4) in matrix form.

$$\mathbf{Q}^{(k)} = \sigma(\mathbf{D}_E^{-1} \mathbf{H}^T \mathbf{P}^{(k-1)} \Theta_E^{(k)} + \mathbf{b}_E^{(k)}), \quad \mathbf{P}^{(k)} = \sigma(\mathbf{D}_V^{-1} \mathbf{H} \mathbf{W} \mathbf{Q}^{(k)} \Theta_V^{(k)} + \mathbf{b}_V^{(k)}), \quad (4)$$

where  $\mathbf{P}^{(0)} = \mathbf{X}$  and  $\mathbf{W}$  is the identity matrix.

**(3) Projection head.** Chen et al. [2020] empirically demonstrates that including a non-linear transformation called projection head which maps representations to another latent space where contrastive loss is applied helps to improve the quality of representations. We also adopt two projection heads denoted by  $g_\phi(\cdot)$  and  $g_\psi(\cdot)$  for projecting node and hyperedge representations, respectively. Both projection heads in our method are implemented with a two-layer MLP and ELU activation [Clevert et al., 2016]. Formally,  $\mathbf{Z}_i := g_\phi(\mathbf{P}_i)$  and  $\mathbf{Y}_i := g_\psi(\mathbf{Q}_i)$ , where  $i = 1, 2$  for two augmented views.

**(4) Tri-directional contrastive loss.** In TriCon framework, we employ three contrastive objectives: (a) *node-level contrast* aims to discriminate the representations of the same node in the two augmented views from other node representations, (b) *group-level contrast* tries to distinguish the representations of the same hyperedge in the two augmented views from other hyperedge representations, and (c) *membership-level contrast* seeks to differentiate a “real” node-hyperedge membership from a “fake” one across the two augmented views. We utilize the InfoNCE loss [Oord et al., 2018], one of the popular contrastive losses, as in [Zhu et al., 2020, 2021, Qiu et al., 2020].

**Node-level contrast.** For any node  $v_i$ , its representation from the first view,  $\mathbf{z}_{1,i}$ , is set to the anchor, the representation of it from the second view,  $\mathbf{z}_{2,i}$ , is treated as the positive sample, and the representations of the other nodes from the second view,  $\mathbf{z}_{2,k}$ , where  $k \neq i$ , are regarded as negative samples. Let  $s(\cdot, \cdot)$  denote the *score* function (a.k.a. *critic* function) that assigns high values to the positive pair, and low values to negative pairs [Tschanne et al., 2019]. We use the cosine similarity as the score (i.e.  $s(\mathbf{u}, \mathbf{v}) = \mathbf{u}^T \mathbf{v} / \|\mathbf{u}\| \|\mathbf{v}\|$ ). Then the loss function for each positive node pair is defined as:

$$\ell_n(\mathbf{z}_{1,i}, \mathbf{z}_{2,i}) = -\log \frac{e^{s(\mathbf{z}_{1,i}, \mathbf{z}_{2,i})/\tau_n}}{e^{s(\mathbf{z}_{1,i}, \mathbf{z}_{2,i})/\tau_n} + \sum_{k=1, k \neq i}^{|V|} e^{s(\mathbf{z}_{1,i}, \mathbf{z}_{2,k})/\tau_n}} = -\log \frac{e^{s(\mathbf{z}_{1,i}, \mathbf{z}_{2,i})/\tau_n}}{\sum_{k=1}^{|V|} e^{s(\mathbf{z}_{1,i}, \mathbf{z}_{2,k})/\tau_n}}, \quad (5)$$

where  $\tau_n$  is a temperature parameter. In practice, we symmetrize this loss by setting the node representation of the second view as the anchor. The objective function for node-level contrast is defined as the average over all positive pairs as:

$$\mathcal{L}_n = \frac{1}{2|V|} \sum_{i=1}^{|V|} \{\ell_n(\mathbf{z}_{1,i}, \mathbf{z}_{2,i}) + \ell_n(\mathbf{z}_{2,i}, \mathbf{z}_{1,i})\}. \quad (6)$$

**Group-level contrast.** For any hyperedge (i.e., a group of nodes)  $e_j$ , its representation from the first view,  $\mathbf{y}_{1,j}$ , is set to the anchor, the representation of it from the second view,  $\mathbf{y}_{2,j}$ , is treated as the positive sample, and the representations of the other hyperedges from the second view,  $\mathbf{y}_{2,k}$ , where  $k \neq j$ , are regarded as negative samples. We also use the cosine similarity as the critic, and then the loss function for each positive hyperedge pair is defined as:

$$\ell_g(\mathbf{y}_{1,j}, \mathbf{y}_{2,j}) = -\log \frac{e^{s(\mathbf{y}_{1,j}, \mathbf{y}_{2,j})/\tau_g}}{e^{s(\mathbf{y}_{1,j}, \mathbf{y}_{2,j})/\tau_g} + \sum_{k=1, k \neq j}^{|E|} e^{s(\mathbf{y}_{1,j}, \mathbf{y}_{2,k})/\tau_g}} = -\log \frac{e^{s(\mathbf{y}_{1,j}, \mathbf{y}_{2,j})/\tau_g}}{\sum_{k=1}^{|E|} e^{s(\mathbf{y}_{1,j}, \mathbf{y}_{2,k})/\tau_g}}, \quad (7)$$

where  $\tau_g$  is a temperature parameter. The objective function for group-level contrast is defined as the average over all positive pairs as:

$$\mathcal{L}_g = \frac{1}{2|E|} \sum_{j=1}^{|E|} \{\ell_g(\mathbf{y}_{1,j}, \mathbf{y}_{2,j}) + \ell_g(\mathbf{y}_{2,j}, \mathbf{y}_{1,j})\}. \quad (8)$$

**Membership-level contrast.** For any node  $v_i$  and hyperedge  $e_j$  that form membership in the original hypergraph, the node representation from the first view,  $\mathbf{z}_{1,i}$ , is set to the anchor, the hyperedge representation from the other view,  $\mathbf{y}_{2,j}$ , is treated as the positive sample. The negative samples are drawn from the other hyperedge representations that are not associated with node  $v_i$ , denoted by  $\mathbf{y}_{2,k}$ , where  $k : i \notin k$ . Symmetrically,  $\mathbf{y}_{2,j}$  can also be the anchor, in which case the negative samples are  $\mathbf{z}_{1,k}$ , where  $k : k \notin j$ . To differentiate a “real” node-hyperedge membership from a “fake” one, we employ a *discriminator*,  $\mathcal{D} : \mathbb{R}^{F'} \times \mathbb{R}^{F''} \rightarrow \mathbb{R}$  as the scoring function, such that  $\mathcal{D}(\mathbf{z}, \mathbf{y})$  represents the probability scores assigned to this node-hyperedge

representation pair (should be higher for “real” pairs) [Hjelm et al., 2019, Veličković et al., 2018a]. For simplicity, we omit the augmented view number in the equation. Then we use the following objective:

$$\ell_m(\mathbf{z}_i, \mathbf{y}_j) = \underbrace{-\log \frac{e^{\mathcal{D}(\mathbf{z}_i, \mathbf{y}_j)/\tau_m}}{e^{\mathcal{D}(\mathbf{z}_i, \mathbf{y}_j)/\tau_m} + \sum_{k:i \neq k} e^{\mathcal{D}(\mathbf{z}_i, \mathbf{y}_k)/\tau_m}}}_{\text{when } \mathbf{z}_i \text{ is the anchor}} - \underbrace{\log \frac{e^{\mathcal{D}(\mathbf{z}_i, \mathbf{y}_j)/\tau_m}}{e^{\mathcal{D}(\mathbf{z}_i, \mathbf{y}_j)/\tau_m} + \sum_{k:k \neq j} e^{\mathcal{D}(\mathbf{z}_k, \mathbf{y}_j)/\tau_m}}}_{\text{when } \mathbf{y}_j \text{ is the anchor}}, \quad (9)$$

where  $\tau_m$  is a temperature parameter. From a practical point of view, considering a large number of negatives poses a prohibitive cost, especially for large graphs [Zhu et al., 2020, Thakoor et al., 2022]. We, therefore, decide to randomly select a single negative sample per positive sample for  $\ell_m(\mathbf{z}_i, \mathbf{y}_j)$ . Since two views are symmetric, we get two node-hyperedge pairs for a single membership, thus the loss for another pair is defined similarly. The objective function for membership-level contrast is the average over all positive node-hyperedge pairs as:

$$\mathcal{L}_m = \frac{1}{2K} \sum_{i=1}^{|V|} \sum_{j=1}^{|E|} \mathbb{1}_{[h_{ij}=1]} \{ \ell_m(\mathbf{z}_{1,i}, \mathbf{y}_{2,j}) + \ell_m(\mathbf{z}_{2,i}, \mathbf{y}_{1,j}) \}. \quad (10)$$

Finally, by integrating Eq. (6), (8), and (10), our proposed tri-directive contrastive loss is formulated as:

$$\mathcal{L} = \mathcal{L}_n + \omega_g \mathcal{L}_g + \omega_m \mathcal{L}_m, \quad (11)$$

where  $\omega_g$  and  $\omega_m$  are the weights of  $\mathcal{L}_g$  and  $\mathcal{L}_m$ , respectively.

To sum up, TriCon jointly optimizes three contrastive objectives: node-, group-, and membership-level contrast, which enable the learned representations of nodes and hyperedges to preserve both the microscopic (i.e., node-level) and mesoscopic (i.e., higher-order) structural information at the same time.

## 4 Experiments

In this section, we empirically evaluate the quality of node representations learnt by TriCon on two hypergraph learning tasks: node classification and clustering, which have been commonly used to benchmark hypergraph learning algorithms [Zhou et al., 2006].

### 4.1 Dataset

We assess the performance of TriCon on a set of 5 commonly used benchmark datasets. Specifically, we use two kinds of standard academic network datasets: (1) co-citation datasets (Cora, Citeseer, and Pubmed) [Sen et al., 2008], (2) co-authorship datasets (Cora and DBLP [Rossi and Ahmed, 2015]). Further descriptions and the statistics of datasets can be found in Appendix A.

### 4.2 Experimental Setup

**Evaluation protocol.** For the node classification task, we follow the standard linear-evaluation protocol as introduced in Veličković et al. [2018a]. Each hypergraph encoder is firstly trained in a fully unsupervised manner and computes node representations; then, a simple linear classifier is trained on top of these frozen representations through a  $\ell_2$ -regularized logistic regression loss, without flowing any gradients back to the hypergraph encoder. For all the datasets, we randomly split them, where 10%, 10%, and 80% of nodes are chosen for the training, validation, and test set, respectively, as has been followed in Zhu et al. [2020], Thakoor et al. [2022]. We evaluate the model with 20 dataset splits over 5 random weight initializations for unsupervised setting, and report the averaged accuracy on each dataset. In a supervised setting, we use 20 dataset splits and a different model initialization for each split and report the averaged accuracy.

For the clustering task, we assess the quality of representations using the k-means clustering by operating it on the frozen node representations produced by each model. We employ the local Lloyd algorithm [Lloyd, 1982] with the k-means++ seeding [Arthur and Vassilvitskii, 2007] approach. For a fair comparison, we train each model with 5 random weight initializations, perform k-means 5 times on each trained encoder, and report the averaged results.

Table 1: Node classification accuracy in percentage along with standard deviations. Graph algorithms, marked as  $\star$ , are applied after converting hypergraphs to graphs via clique expansion. For each dataset, the highest and the second-highest performance is highlighted in **boldface** and underlined, respectively. A.R. denotes average rank, and OOM indicates out of memory on a 24GB GPU.

Method	Co-citation Data			Co-authorship Data		A.R. $\downarrow$	
	Cora	Citeseer	Pubmed	Cora	DBLP		
Supervised	MLP	$60.32 \pm 1.50$	$62.06 \pm 2.27$	$76.27 \pm 1.06$	$64.05 \pm 1.39$	$81.18 \pm 0.18$	14.6
	GCN $\star$	$77.11 \pm 1.84$	$66.07 \pm 2.39$	$82.63 \pm 0.63$	$73.66 \pm 1.34$	$87.58 \pm 0.22$	9.8
	GAT $\star$	$77.75 \pm 2.08$	$67.62 \pm 2.48$	$81.96 \pm 0.74$	$74.52 \pm 1.34$	$88.59 \pm 0.14$	8
	HGNN	$77.50 \pm 1.82$	$66.16 \pm 2.33$	$83.52 \pm 0.67$	$74.38 \pm 1.23$	$88.32 \pm 0.27$	8.2
	HyperConv	$76.19 \pm 2.06$	$64.12 \pm 2.58$	$83.42 \pm 0.61$	$73.52 \pm 1.04$	$88.83 \pm 0.17$	9.4
	HNHN	$76.21 \pm 1.71$	$67.28 \pm 2.19$	$80.97 \pm 0.88$	$74.88 \pm 1.61$	$86.71 \pm 1.24$	9.6
	HyperGCN	$64.11 \pm 7.42$	$59.92 \pm 9.60$	$78.40 \pm 9.21$	$60.65 \pm 9.18$	$76.59 \pm 7.60$	15
	HyperSAGE	$64.98 \pm 5.32$	$52.43 \pm 9.38$	$79.49 \pm 8.68$	$64.59 \pm 4.34$	$79.63 \pm 8.55$	14.2
	UniGCN	$77.91 \pm 1.87$	$66.40 \pm 1.90$	$84.08 \pm 0.66$	$77.30 \pm 1.35$	$90.31 \pm 0.15$	5.4
Unsupervised	Node2vec $\star$	$70.99 \pm 1.43$	$53.85 \pm 1.94$	$78.75 \pm 0.89$	$58.50 \pm 2.09$	$72.09 \pm 0.27$	15.2
	DGI $\star$	$78.17 \pm 1.38$	$68.81 \pm 1.82$	$80.83 \pm 0.59$	$76.94 \pm 1.06$	$88.00 \pm 0.17$	7
	GRACE $\star$	$79.11 \pm 1.72$	$68.65 \pm 1.67$	$80.08 \pm 0.66$	$76.59 \pm 1.00$	OOM	7
	S <sup>2</sup> -HHGR	$78.08 \pm 1.71$	$68.21 \pm 1.80$	$82.13 \pm 0.57$	$78.15 \pm 1.13$	$88.69 \pm 0.15$	6
Unsupervised	Random-Init	$63.62 \pm 3.13$	$60.44 \pm 2.48$	$67.49 \pm 2.23$	$66.27 \pm 2.16$	$76.57 \pm 0.57$	15
	TriCon-N	$80.23 \pm 1.23$	$70.28 \pm 1.50$	$83.44 \pm 0.62$	$81.94 \pm 1.06$	$90.88 \pm 0.12$	3.4
	TriCon-NG	$81.45 \pm 1.22$	$71.38 \pm 1.18$	$83.68 \pm 0.68$	$82.00 \pm 0.99$	$90.94 \pm 0.09$	<u>2.2</u>
	TriCon	<b><math>81.57 \pm 1.12</math></b>	<b><math>72.02 \pm 1.16</math></b>	<b><math>84.26 \pm 0.62</math></b>	<b><math>82.15 \pm 0.89</math></b>	<b><math>91.12 \pm 0.11</math></b>	<b>1</b>

**Baselines.** We compare our proposed method with various representative baseline approaches including 9 (semi-)supervised models and 4 unsupervised models. A detailed description of these baselines is provided in Appendix B. Note that, since the methods working on graphs can not be directly applied to hypergraphs, we use them after transforming hypergraphs to graphs via clique expansion. For all baselines, we report their performance based on their official implementations.

**Implementation details.** We employ a one-layer mean pooling hypergraph encoder described in (4) and PReLU [He et al., 2015] activation for non-linearity. Following Tschannen et al. [2019], which has experimentally shown a simple bilinear critic yields better downstream performance than higher-capacity MLP critics, we use a bilinear function as a discriminator to score node-hyperedge representation pairs, formulated as  $\mathcal{D}(\mathbf{z}, \mathbf{y}) = \sigma(\mathbf{z}^T \mathbf{S} \mathbf{y})$ . Here,  $\mathbf{S}$  denotes a trainable scoring matrix and  $\sigma$  is the sigmoid function to transform scores into probabilities of  $(\mathbf{z}, \mathbf{y})$  being a positive sample. A description of the optimizer and model hyperparameters are provided in Appendix C.

### 4.3 Performance on Node Classification

Table 1 summarizes the empirical performance of all methods. Overall, as can be seen from the table, our proposed method achieves the strongest performance across all datasets. TriCon consistently outperforms its unsupervised baselines by significant margins, and also outperforms the models trained with label supervision. Below, we make three notable observations.

First, applying graph learning algorithms on hypergraph datasets is less effective. The graph contrastive learning methods like Node2vec, DGI, and GRACE show significant lower accuracy compared to TriCon, especially in the Pubmed and Cora Co-authorship datasets. This is because converting hypergraphs to graphs via clique expansion involves a loss of structural information [Hein et al., 2013, Li and Milenkovic, 2018, Dong et al., 2020]. As these two datasets have large maximum and average hyperedge sizes (see Appendix A), the amount of information loss increases, leading to significant performance degradation.

Second, rather than just using node-level contrast, considering the different types of contrast (i.e., group- and membership-level contrast) together can help improve performance. We propose and evaluate two model variants, denoted as TriCon-N and TriCon-NG, which use only node-level contrast and node- and group-level contrast, respectively, to validate the effect of each type of contrast. From Table 1, we note that the more types of contrast we use, the better the performance is. To be more specific, we analyze the effectiveness

Table 2: Comparison of node classification accuracy according to whether or not to use each type of contrast (i.e.,  $\mathcal{L}_n$ ,  $\mathcal{L}_g$ , and  $\mathcal{L}_m$ ). Using all types of contrasts (i.e., node-, group-, and membership-level contrast) achieves the best performance as they are complementary reinforcing each other.

$\mathcal{L}_n$	$\mathcal{L}_g$	$\mathcal{L}_m$	Co-citation Data			Co-authorship Data		A.R. $\downarrow$
			Cora	Citeseer	Pubmed	Cora	DBLP	
✓	-	-	80.23 $\pm$ 1.23	<u>70.28 <math>\pm</math> 1.47</u>	83.44 $\pm$ 0.62	81.94 $\pm$ 1.06	90.88 $\pm$ 0.12	4.2
-	✓	-	79.69 $\pm$ 1.62	<u>71.02 <math>\pm</math> 1.29</u>	80.20 $\pm$ 1.30	78.98 $\pm$ 1.39	88.60 $\pm$ 0.21	5.6
-	-	✓	76.76 $\pm$ 1.83	63.98 $\pm$ 2.03	79.86 $\pm$ 0.89	76.77 $\pm$ 1.10	63.95 $\pm$ 7.19	7
✓	✓	-	<u>81.45 <math>\pm</math> 1.22</u>	71.38 $\pm$ 1.37	83.68 $\pm$ 0.68	<u>82.00 <math>\pm</math> 0.99</u>	<u>90.94 <math>\pm</math> 0.09</u>	<u>2.4</u>
✓	-	✓	80.49 $\pm$ 1.36	70.46 $\pm$ 1.51	<u>83.98 <math>\pm</math> 0.65</u>	81.62 $\pm$ 1.03	90.75 $\pm$ 0.12	3.8
-	✓	✓	80.80 $\pm$ 1.18	<u>71.73 <math>\pm</math> 1.44</u>	82.81 $\pm$ 0.73	80.24 $\pm$ 0.99	90.17 $\pm$ 0.14	4
✓	✓	✓	<b>81.57 <math>\pm</math> 1.12</b>	<b>72.02 <math>\pm</math> 1.39</b>	<b>84.26 <math>\pm</math> 0.62</b>	<b>82.15 <math>\pm</math> 0.89</b>	<b>91.12 <math>\pm</math> 0.11</b>	<b>1</b>

Table 3: TriCon is very robust to the number of negative samples (i.e.,  $k$ ). A.P.D. denotes average performance degradation. Even if only two negative samples are used at every gradient step, the performance degrades by less than 1%.

Method	Co-citation Data			Co-authorship Data		A.P.D.
	Cora	Citeseer	Pubmed	Cora	DBLP	
S <sup>2</sup> -HHGR all negatives	78.08 $\pm$ 1.71	68.21 $\pm$ 1.80	82.13 $\pm$ 0.57	78.15 $\pm$ 1.13	88.69 $\pm$ 0.15	-
TriCon-Subsampling ( $k = 2$ )	80.62 $\pm$ 1.29	71.95 $\pm$ 1.27	83.22 $\pm$ 0.70	81.25 $\pm$ 1.03	90.66 $\pm$ 0.15	0.82%
TriCon-Subsampling ( $k = 4$ )	81.15 $\pm$ 1.20	<b>72.24 <math>\pm</math> 1.18</b>	83.91 $\pm$ 0.68	81.85 $\pm$ 0.91	90.83 $\pm$ 0.11	0.26%
TriCon-Subsampling ( $k = 8$ )	81.32 $\pm$ 1.19	72.04 $\pm$ 1.26	83.88 $\pm$ 0.68	82.05 $\pm$ 0.87	90.93 $\pm$ 0.11	0.21%
TriCon-Subsampling ( $k = 16$ )	81.49 $\pm$ 1.14	72.02 $\pm$ 1.15	84.23 $\pm$ 0.65	82.10 $\pm$ 0.87	90.97 $\pm$ 0.12	0.07%
TriCon all negatives	<b>81.57 <math>\pm</math> 1.12</b>	72.02 $\pm$ 1.16	<b>84.26 <math>\pm</math> 0.62</b>	<b>82.15 <math>\pm</math> 0.89</b>	<b>91.12 <math>\pm</math> 0.11</b>	-

of each type of contrast (i.e.,  $\mathcal{L}_n$ ,  $\mathcal{L}_g$ , and  $\mathcal{L}_m$ ) on the node classification task in Table 2. We conduct experiments on all combinations of all types of contrast. The results show that using all types of contrast achieves the best performance as they are complementary reinforcing each other. In most cases, using a combination of any two types of contrast is more powerful than using only one. It is noteworthy that while membership-level contrast causes model collapse (especially for the Citeseer and DBLP datasets) when used alone, it boosts performance when used with node- or group-level contrast.

Finally, in Table 2, we note that group-level contrast is more crucial than node-level contrast for the Citeseer dataset (highlighted with a wavy line), even though the downstream task is node-level.

To sum up, the superior performance of TriCon demonstrates that it produces highly generalized representations. Additional analysis and discussion on the impact of hyperparameters in TriCon are provided in Appendix E.

**Robustness to the number of negatives.** To analyze how the number of negative samples influences the node classification performance, we propose an approximation of TriCon’s objective called TriCon-Subsampling. Here, instead of constructing the contrastive loss with all negatives, we randomly subsample  $k$  negatives across the hypergraph for node- and group-level contrast, respectively, at every gradient step. Our results in Table 3 show that TriCon is very robust to the number of negatives; even if only two negative samples are used for node- and group-level contrast, the performance degradation is less than 1%, still outperforming the best performing unsupervised baseline method, S<sup>2</sup>-HHGR, by great margins. Additionally, the results indicate that the random negative sampling is sufficiently effective for TriCon, and there is no need to select hard negatives, which incur additional costs.

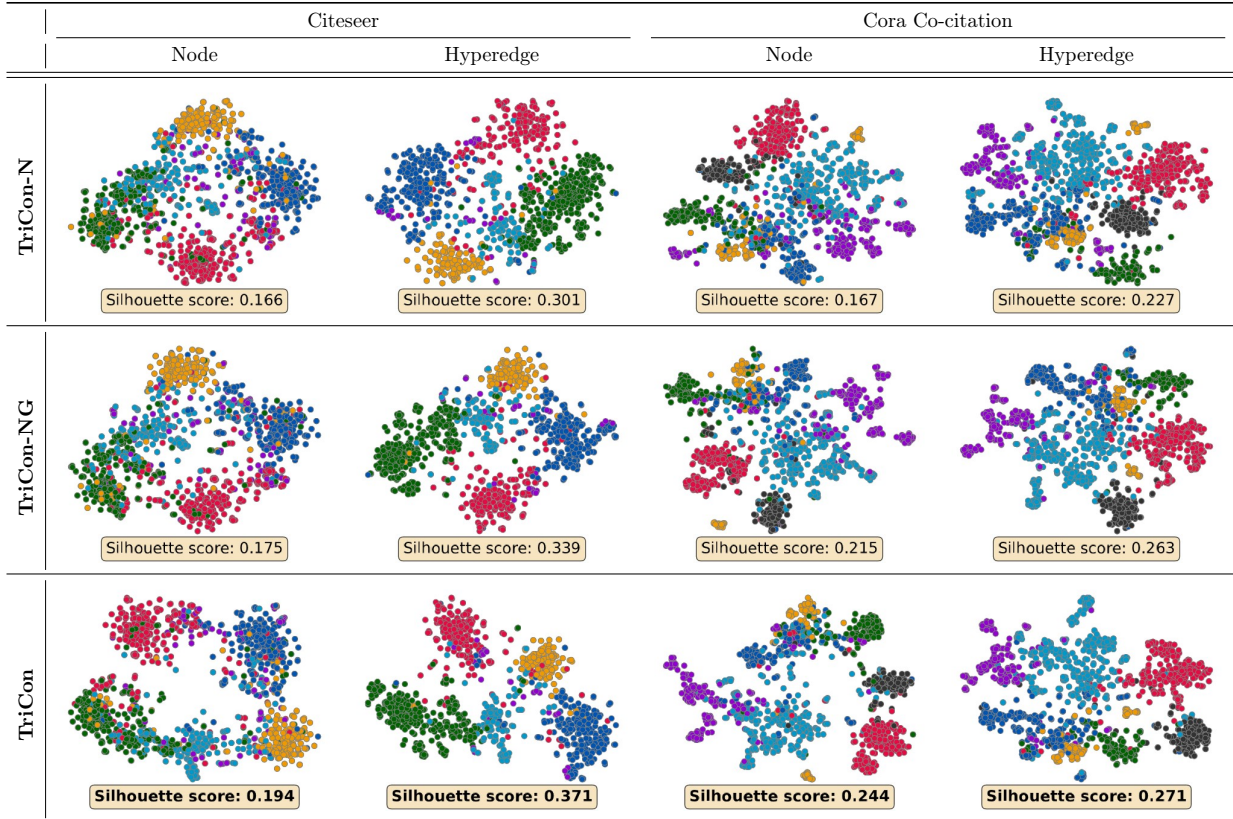
#### 4.4 Performance on Clustering

To show how well node representations trained with TriCon generalize across various downstream tasks, we evaluate the representations on the clustering task by k-means as described in Section 4.2. We use the node labels as ground truth for the clusters. To evaluate the clusters generated by k-means, we measure the agreement between the true labels and the cluster assignments by three metrics: Completeness Score

Table 4: Evaluation of the representations learned by unsupervised methods using k-means clustering. As a naïve baseline method, expressed by ‘features’, we only use the node features as an input of k-means. All metrics are normalized by multiplying 100. TriCon ranks first in clustering performance. Larger CS, NMI, and F1 indicate better performance, and A.R. denotes average ranking.

Method	Cora Co-citation			Citeseer			Pubmed			Cora Co-authorship			DBLP			A.R.↓
	CS↑	NMI↑	F1↑	CS↑	NMI↑	F1↑	CS↑	NMI↑	F1↑	CS↑	NMI↑	F1↑	CS↑	NMI↑	F1↑	
features	20.2	20.0	28.8	21.8	21.5	36.1	22.5	19.5	<b>53.4</b>	18.1	17.2	29.2	37.7	37.0	47.3	5.1
Node2vec*	39.4	39.1	44.5	27.8	24.5	38.5	23.3	23.1	40.1	18.4	16.0	34.1	36.8	32.4	37.8	5.1
DGI*	<b>55.1</b>	<b>54.8</b>	<b>60.1</b>	40.4	40.1	51.7	<b>30.6</b>	<b>30.4</b>	53.0	45.0	45.2	<b>52.5</b>	58.6	58.0	57.7	<b>2.3</b>
GRACE*	45.6	44.4	45.6	33.4	33.3	45.7	17.2	16.7	41.9	37.9	37.9	43.3	17.2	16.7	41.9	4.7
S <sup>2</sup> -HHGR	50.2	51.0	56.8	<b>41.0</b>	<b>41.1</b>	<b>53.1</b>	27.4	27.7	<b>53.2</b>	<b>44.6</b>	<b>45.4</b>	52.3	<b>60.3</b>	<b>60.3</b>	<b>62.7</b>	2.5
<b>TriCon</b>	<b>54.4</b>	<b>54.5</b>	<b>60.6</b>	<b>44.1</b>	<b>44.1</b>	<b>57.4</b>	<b>30.6</b>	<b>30.0</b>	51.7	<b>49.1</b>	<b>49.8</b>	<b>56.7</b>	<b>64.8</b>	<b>63.1</b>	<b>63.0</b>	<b>1.4</b>

Table 5: t-SNE plots of the node and hyperedge representations from TriCon and its two variants. The TriCon’s embeddings exhibits the most distinct clusters with the help of group and membership contrast, as measured by the Silhouette score (the higher, the better).



(CS), Normalized Mutual Information (NMI), and pairwise F1 score. Table 4 summarizes the empirical performance. Our results show that TriCon achieves strong clustering performance in terms of all metrics across all datasets (1st place in terms of the average ranking). This is because the node embeddings learned by TriCon simultaneously preserve local and community structural information by actively utilizing group- and membership-level contrast. Interestingly, DGI also shows relatively solid performance compared to other baseline approaches, because it is trained to maximize the mutual information between the local node-level and global graph-level embeddings. This also makes embeddings retain local and global structural information.

## 4.5 Qualitative Analysis

To represent and compare the quality of embeddings intuitively, Table 5 shows t-SNE [Van der Maaten and Hinton, 2008] plots of the node and hyperedge embeddings produced by TriCon and its two variants (i.e., TriCon-N and TriCon-NG) on the Citeseer and Cora Co-citation dataset. Note that the label of the hyperedge is assigned to the most dominant label by counting the labels of neighbor nodes within two hops, and if the counts of some labels are equal, it is randomly selected among them. As expected from the quantitative results, the 2-D projection of embeddings learned by TriCon shows more visually and numerically (based on Silhouette score [Rousseeuw, 1987]) distinguishable clusters than its two variants. In Appendix F, we give additional qualitative analysis.

## 5 Conclusion

In this paper, we proposed TriCon, a novel hypergraph contrastive representation learning approach. We summarize our contributions as follows:

- We proposed the use of tri-directional contrast, which is a combination of node-, group-, and membership-level contrast, that consistently and substantially improves the quality of the learned representations.
- We achieved state-of-the-art results in node classification on hypergraphs by using tri-directional contrast together with our data augmentation schemes. Moreover, we verified the surprising effectiveness of uniform negative sampling for our use cases.
- We demonstrated the superiority of TriCon by conducting extensive experiments using 13 baseline approaches, five datasets, and two tasks.

## References

Austin R Benson, Rediet Abebe, Michael T Schaub, Ali Jadbabaie, and Jon Kleinberg. Simplicial closure and higher-order link prediction. *Proceedings of the National Academy of Sciences*, 115(48), 2018.

Manh Tuan Do, Se-eun Yoon, Bryan Hooi, and Kijung Shin. Structural patterns and generative models of real-world hypergraphs. In *Proceedings of the 26th ACM SIGKDD International Conference on Knowledge Discovery & Data Mining*, 2020.

Geon Lee, Jihoon Ko, and Kijung Shin. Hypergraph motifs: concepts, algorithms, and discoveries. In *Proceedings of the VLDB Endowment*, 2020.

Dingqi Yang, Bingqing Qu, Jie Yang, and Philippe Cudre-Mauroux. Revisiting user mobility and social relationships in lbsns: a hypergraph embedding approach. In *The World Wide Web Conference*, 2019.

Xin Xia, Hongzhi Yin, Junliang Yu, Qinyong Wang, Lizhen Cui, and Xiangliang Zhang. Self-supervised hypergraph convolutional networks for session-based recommendation. In *Proceedings of the AAAI Conference on Artificial Intelligence*, 2021.

Xiao Zheng, Wenyang Zhu, Chang Tang, and Minhui Wang. Gene selection for microarray data classification via adaptive hypergraph embedded dictionary learning. *Gene*, 706:188–200, 2019.

Yifan Feng, Haoxuan You, Zizhao Zhang, Rongrong Ji, and Yue Gao. Hypergraph neural networks. In *Proceedings of the AAAI Conference on Artificial Intelligence*, 2019.

Austin R Benson, David F Gleich, and Jure Leskovec. Higher-order organization of complex networks. *Science*, 353(6295):163–166, 2016.

Junliang Yu, Hongzhi Yin, Jundong Li, Qinyong Wang, Nguyen Quoc Viet Hung, and Xiangliang Zhang. Self-supervised multi-channel hypergraph convolutional network for social recommendation. In *Proceedings of the Web Conference*, 2021.

Geon Lee, Minyoung Choe, and Kijung Shin. Hashnwalk: Hash and random walk based anomaly detection in hyperedge streams. In *International Joint Conferences on Artificial Intelligence Organization*, 2022.

Naganand Yadati, Madhav Nimishakavi, Prateek Yadav, Vikram Nitin, Anand Louis, and Partha Talukdar. Hypergen: A new method for training graph convolutional networks on hypergraphs. In *Advances in Neural Information Processing Systems*, 2019.

Yihe Dong, Will Sawin, and Yoshua Bengio. Hnbn: Hypergraph networks with hyperedge neurons. In *ICML Workshop on Graph Representation Learning and Beyond*, 2020.

Song Bai, Feihu Zhang, and Philip HS Torr. Hypergraph convolution and hypergraph attention. *Pattern Recognition*, 110:107637, 2021.

Devanshu Arya, Deepak K Gupta, Stevan Rudinac, and Marcel Worring. Hypersage: Generalizing inductive representation learning on hypergraphs. *arXiv:2010.04558*, 2020.

Yu Rong, Wenbing Huang, Tingyang Xu, and Junzhou Huang. Dropedge: Towards deep graph convolutional networks on node classification. In *International Conference on Learning Representations*, 2020.

Yixin Liu, Ming Jin, Shirui Pan, Chuan Zhou, Yu Zheng, Feng Xia, and Philip Yu. Graph self-supervised learning: A survey. *IEEE Transactions on Knowledge and Data Engineering*, 2022.

Ashish Jaiswal, Ashwin Ramesh Babu, Mohammad Zaki Zadeh, Debapriya Banerjee, and Fillia Makedon. A survey on contrastive self-supervised learning. *Technologies*, 9(1):2, 2020.

Xiao Liu, Fanjin Zhang, Zhenyu Hou, Li Mian, Zhaoyu Wang, Jing Zhang, and Jie Tang. Self-supervised learning: Generative or contrastive. *IEEE Transactions on Knowledge and Data Engineering*, 2021.

Ting Chen, Simon Kornblith, Mohammad Norouzi, and Geoffrey Hinton. A simple framework for contrastive learning of visual representations. In *International Conference on Machine Learning*, 2020.

R Devon Hjelm, Alex Fedorov, Samuel Lavoie-Marchildon, Karan Grewal, Phil Bachman, Adam Trischler, and Yoshua Bengio. Learning deep representations by mutual information estimation and maximization. In *International Conference on Learning Representations*, 2019.

Tianyu Gao, Xingcheng Yao, and Danqi Chen. Simcse: Simple contrastive learning of sentence embeddings. In *Conference on Empirical Methods in Natural Language Processing*, 2021.

Petar Veličković, William Fedus, William L Hamilton, Pietro Liò, Yoshua Bengio, and R Devon Hjelm. Deep graph infomax. In *International Conference on Learning Representations*, 2018a.

Zhen Peng, Wenbing Huang, Minnan Luo, Qinghua Zheng, Yu Rong, Tingyang Xu, and Junzhou Huang. Graph representation learning via graphical mutual information maximization. In *Proceedings of The Web Conference*, 2020.

Kaveh Hassani and Amir Hosein Khasahmadi. Contrastive multi-view representation learning on graphs. In *International Conference on Machine Learning*, 2020.

Yanqiao Zhu, Yichen Xu, Feng Yu, Qiang Liu, Shu Wu, and Liang Wang. Deep graph contrastive representation learning. In *ICML Workshop on Graph Representation Learning and Beyond*, 2020.

Yanqiao Zhu, Yichen Xu, Feng Yu, Qiang Liu, Shu Wu, and Liang Wang. Graph contrastive learning with adaptive augmentation. In *Proceedings of the Web Conference*, 2021.

Yuning You, Tianlong Chen, Yongduo Sui, Ting Chen, Zhangyang Wang, and Yang Shen. Graph contrastive learning with augmentations. In *Advances in Neural Information Processing Systems*, 2020.

Junwei Zhang, Min Gao, Junliang Yu, Lei Guo, Jundong Li, and Hongzhi Yin. Double-scale self-supervised hypergraph learning for group recommendation. In *Proceedings of the 30th ACM International Conference on Information & Knowledge Management (CIKM)*, 2021.

Matthias Hein, Simon Setzer, Leonardo Jost, and Syama Sundar Rangapuram. The total variation on hypergraphs-learning on hypergraphs revisited. In *Advances in Neural Information Processing Systems*, 2013.

Pan Li and Olgica Milenkovic. Submodular hypergraphs: p-laplacians, cheeger inequalities and spectral clustering. In *International Conference on Machine Learning*, 2018.

Jing Huang and Jie Yang. Unignn: a unified framework for graph and hypergraph neural networks. In *International Joint Conferences on Artificial Intelligence Organization*, 2021.

Jiying Zhang, Fuyang Li, Xi Xiao, Tingyang Xu, Yu Rong, Junzhou Huang, and Yatao Bian. Hypergraph convolutional networks via equivalency between hypergraphs and undirected graphs. *arXiv:2203.16939*, 2022.

Eli Chien, Chao Pan, Jianhao Peng, and Olgica Milenkovic. You are allset: A multiset function framework for hypergraph neural networks. In *International Conference on Learning Representations*, 2022.

Manzil Zaheer, Satwik Kottur, Siamak Ravanbakhsh, Barnabas Poczos, Russ R Salakhutdinov, and Alexander J Smola. Deep sets. In *Advances in Neural Information Processing Systems*, 2017.

Juho Lee, Yoonho Lee, Jungtaek Kim, Adam Kosiorek, Seungjin Choi, and Yee Whye Teh. Set transformer: A framework for attention-based permutation-invariant neural networks. In *International Conference on Machine Learning*, 2019.

Kaiming He, Haoqi Fan, Yuxin Wu, Saining Xie, and Ross Girshick. Momentum contrast for unsupervised visual representation learning. In *Proceedings of the IEEE Conference on Computer Vision and Pattern Recognition*, 2020.

Bryan Perozzi, Rami Al-Rfou, and Steven Skiena. Deepwalk: Online learning of social representations. In *Proceedings of the 20th ACM SIGKDD International Conference on Knowledge Discovery and Data Mining*, 2014.

Aditya Grover and Jure Leskovec. node2vec: Scalable feature learning for networks. In *Proceedings of the 22nd ACM SIGKDD International Conference on Knowledge Discovery and Data Mining*, 2016.

William L Hamilton, Rex Ying, and Jure Leskovec. Representation learning on graphs: Methods and applications. *IEEE Data Engineering Bulletin*, 2017.

Shantanu Thakoor, Corentin Tallec, Mohammad Gheshlaghi Azar, Mehdi Azabou, Eva L Dyer, Remi Munos, Petar Veličković, and Michal Valko. Large-scale representation learning on graphs via bootstrapping. In *International Conference on Learning Representations*, 2022.

Djork-Arné Clevert, Thomas Unterthiner, and Sepp Hochreiter. Fast and accurate deep network learning by exponential linear units (elus). In *International Conference on Learning Representations*, 2016.

Aaron van den Oord, Yazhe Li, and Oriol Vinyals. Representation learning with contrastive predictive coding. *arXiv:1807.03748*, 2018.

Jiezhong Qiu, Qibin Chen, Yuxiao Dong, Jing Zhang, Hongxia Yang, Ming Ding, Kuansan Wang, and Jie Tang. Gcc: Graph contrastive coding for graph neural network pre-training. In *Proceedings of the 26th ACM SIGKDD International Conference on Knowledge Discovery & Data Mining*, 2020.

Michael Tschannen, Josip Djolonga, Paul K Rubenstein, Sylvain Gelly, and Mario Lucic. On mutual information maximization for representation learning. In *International Conference on Learning Representations*, 2019.

Dengyong Zhou, Jiayuan Huang, and Bernhard Schölkopf. Learning with hypergraphs: Clustering, classification, and embedding. *Advances in Neural Information Processing Systems*, 2006.

Prithviraj Sen, Galileo Namata, Mustafa Bilgic, Lise Getoor, Brian Galligher, and Tina Eliassi-Rad. Collective classification in network data. *AI magazine*, 29(3):93–93, 2008.

Ryan Rossi and Nesreen Ahmed. The network data repository with interactive graph analytics and visualization. In *Proceedings of the AAAI Conference on Artificial Intelligence*, 2015.

Stuart Lloyd. Least squares quantization in pcm. *IEEE Transactions on Information Theory*, 28(2):129–137, 1982.

David Arthur and Sergei Vassilvitskii. k-means++: The advantages of careful seeding. In *Proceedings of the Eighteenth Annual ACM-SIAM Symposium on Discrete Algorithms*, 2007.

Kaiming He, Xiangyu Zhang, Shaoqing Ren, and Jian Sun. Delving deep into rectifiers: Surpassing human-level performance on imagenet classification. In *IEEE/CVF International Conference on Computer Vision*, 2015.

Laurens Van der Maaten and Geoffrey Hinton. Visualizing data using t-sne. *Journal of Machine Learning Research*, 9(11), 2008.

Peter J Rousseeuw. Silhouettes: a graphical aid to the interpretation and validation of cluster analysis. *Journal of Computational and Applied Mathematics*, 20:53–65, 1987.

Thomas N Kipf and Max Welling. Semi-supervised classification with graph convolutional networks. In *International Conference on Learning Representations*, 2017.

Petar Veličković, Guillem Cucurull, Arantxa Casanova, Adriana Romero, Pietro Liò, and Yoshua Bengio. Graph attention networks. In *International Conference on Learning Representations*, 2018b.

Adam Paszke, Sam Gross, Francisco Massa, Adam Lerer, James Bradbury, Gregory Chanan, Trevor Killeen, Zeming Lin, Natalia Gimelshein, Luca Antiga, et al. Pytorch: An imperative style, high-performance deep learning library. In *Advances in Neural Information Processing Systems*, 2019.

Matthias Fey and Jan Eric Lenssen. Fast graph representation learning with pytorch geometric. *arXiv:1903.02428*, 2019.

Xavier Glorot and Yoshua Bengio. Understanding the difficulty of training deep feedforward neural networks. In *International Conference on Artificial Intelligence and Statistics*, 2010.

Diederik P Kingma and Jimmy Ba. Adam: A method for stochastic optimization. In *International Conference on Learning Representations*, 2015.

Ilya Loshchilov and Frank Hutter. Decoupled weight decay regularization. In *International Conference on Learning Representations*, 2019.

Feng Wang and Huaping Liu. Understanding the behaviour of contrastive loss. In *Proceedings of the IEEE Conference on Computer Vision and Pattern Recognition*, 2021.

## A Dataset Details

We use two kinds of standard academic network datasets: (1) co-citation datasets (Cora, Citeseer, and Pubmed)<sup>1</sup> [Sen et al., 2008], (2) co-authorship datasets (Cora<sup>2</sup> and DBLP<sup>3</sup> [Rossi and Ahmed, 2015]). Some basic statistics of the datasets used in our experiments are provided in Table 6.

The co-citation datasets are composed of a set of papers and their citation links. To represent a co-citation relationship as a hypergraph, papers become nodes and citation links become hyperedges. To be specific, the nodes  $v_1, \dots, v_k$  compose a hyperedge  $e$  when the papers corresponding to  $v_1, \dots, v_k$  are referred by the document  $e$ . The co-authorship datasets are composed of a set of papers with their authors. In hypergraphs that model the co-authorship datasets, nodes and hyperedges represent papers and authors, respectively. Precisely, the nodes  $v_1, \dots, v_k$  compose a hyperedge  $e$  when the papers corresponding to  $v_1, \dots, v_k$  are written by the author  $e$ . Features of each node are represented by bag-of-words features from its abstract. Nodes are labeled with their categories.

The hypergraphs preprocessed from all the datasets are publicly available with the official implementation of HyperGCN<sup>4</sup> [Yadati et al., 2019]. Additionally, we remove nodes that are not included in any hyperedge (i.e. isolated nodes) from the hypergraphs, because such nodes cause trivial structures in hypergraphs and their predictions would only depend on the features of that node. For all the datasets, we randomly select 10%, 10%, and 80% of nodes disjointly for the training, validation, and test sets, respectively. The datasets and train-valid-test splits used in our experiments are provided as supplementary materials.

Table 6: Statistics of datasets used in our experiments.

	Co-citation Data			Co-authorship Data	
	Cora	Citeseer	Pubmed	Cora	DBLP
# Nodes	1,434	1,458	3,840	2,388	41,302
# Hyperedges	1,579	1,079	7,963	1,072	22,363
# Node-hyperedge connections	4,786	3,453	34,629	4,585	99,561
Avg. hyperedge size	$3.03 \pm 1.02$	$3.20 \pm 2.02$	$4.35 \pm 5.67$	$4.28 \pm 4.24$	$4.45 \pm 5.42$
Avg. node degree	$3.34 \pm 5.96$	$2.37 \pm 3.61$	$9.02 \pm 8.16$	$1.92 \pm 1.32$	$2.41 \pm 1.24$
Max. hyperedge size	5	26	171	43	202
Max. node degree	145	88	99	23	18
# Features	1,433	3,703	500	1,433	1,425
# Classes	7	6	3	7	6

## B Baseline Details

We compare our proposed method with various representative baseline approaches that can be categorized into (1) supervised learning methods (GCN [Kipf and Welling, 2017] and GAT [Veličković et al., 2018b] applied to graphs and HGNN [Feng et al., 2019], HyperConv [Bai et al., 2021], HNHN [Dong et al., 2020], HyperGCN [Yadati et al., 2019], HyperSAGE [Arya et al., 2020], and UniGCN [Huang and Yang, 2021] applied directly to hypergraphs), and (2) unsupervised learning methods (Node2vec [Grover and Leskovec, 2016], DGI [Veličković et al., 2018a], and GRACE [Zhu et al., 2020], which are representative graph contrastive learning methods and S<sup>2</sup>-HHGR [Zhang et al., 2021], which is a hypergraphs contrastive learning method). To measure the quality of the inductive biases inherent in the encoder model, we also consider Random-Init [Veličković et al., 2018a, Thakoor et al., 2022], an encoder with the same architecture as TriCon but with randomly initialized parameters, as a baseline. Since the methods working on graphs can not be directly applied to hypergraphs, we use them after transforming hypergraphs to graphs via clique expansion. In the case of S<sup>2</sup>-HHGR, it is originally designed for group recommendations with supervisory signals, and therefore it is not directly applicable to node classification tasks. Thus we slightly modified the algorithm so that it uses only its self-supervised loss. For all the baseline approaches, we report their performance using their official implementations.

<sup>1</sup><https://linqs.soe.ucsc.edu/data>

<sup>2</sup><https://people.cs.umass.edu/~mccallum/data.html>

<sup>3</sup><https://aminer.org/lab-datasets/citation/DBLP-citation-Jan8.tar.bz>

<sup>4</sup><https://github.com/malllabiisc/HyperGCN>

## C Implementation Details

### C.1 Infrastructures and Implementations

All experiments are performed on a server with NVIDIA RTX 3090 Ti GPUs (24GB memory), 256GB of RAM, and two Intel Xeon Silver 4210R Processors. Our models are implemented using PyTorch 1.11.0 [Paszke et al., 2019] and PyTorch Geometric 2.0.4 [Fey and Lenssen, 2019].

### C.2 Hyperparameters

As described in Section 4.2, we use a one-layer mean pooling hypergraph encoder as in Eq. (4) and PReLU [He et al., 2015] activation in all the experiments. Note that, to each node, we add a self-loop which is a hyperedge which contains exactly one node, before the hypergraph is fed into the encoder. In Appendix E.1, we show that adding self-loops helps to improve the quality of representations. Self-loops and empty-hyperedges (i.e., hyperedges with degree zero) are ignored when constructing the proposed tri-directional contrastive loss.

In all our experiments, all models are initialized with Glorot initialization [Glorot and Bengio, 2010] and trained using the AdamW optimizer [Kingma and Ba, 2015, Loshchilov and Hutter, 2019] with weight decay set to  $10^{-5}$ . We train the model for a fixed number of epochs at which the performance of node classification sufficiently converges.

The augmentation hyperparameters  $p_f$  and  $p_m$ , which control the sampling process for node feature and membership masking, respectively, are chosen between 0.0 and 0.4 so that the original hypergraph is not overly corrupted. Some prior works [Zhu et al., 2020, 2021] have demonstrated that using a different degree of augmentation for each view shows better results, and we can also adopt different hyperparameters for each augmented view (as mentioned in Section 3.3). However, our contributions are orthogonal to this problem, thus we choose the same hyperparameters for two augmented views (i.e.,  $p_{f,1} = p_{f,2} = p_f$  and  $p_{m,1} = p_{m,2} = p_m$ ) for simplicity. In Appendix D, we demonstrate that using node feature masking and membership masking together is a reasonable choice.

The three temperature hyperparameters  $\tau_n$ ,  $\tau_g$ , and  $\tau_m$ , which control the uniformity of the embedding distribution [Wang and Liu, 2021], are selected from 0.1 to 1.0, respectively. The weights  $\omega_g$  and  $\omega_m$  are chosen from  $[2^{-4}, 2^{-3}, \dots, 2^4]$ , respectively. The size of node embeddings, hyperedge embeddings, and a hidden layer of projection heads are set to 512 with an exception to 256 on the DBLP dataset. In Table 7, we provide hyperparameters we found through a small grid search based on the validation accuracy, as many self-supervised learning methods do [Chen et al., 2020, Zhu et al., 2020, 2021, Thakoor et al., 2022].

Table 7: Hyperparameter settings on each dataset. Cora-C and Cora-A stand for Cora Co-citation and Cora Co-authorship, respectively.

Dataset	$p_f$	$p_m$	$\tau_n$	$\tau_g$	$\tau_m$	$\omega_g$	$\omega_m$	Learning Rate	Training Epochs	Node Emb. Size	Hyperedge Emb. Size	Projection Hidden Size
Cora-C	0.4	0.4	0.5	0.5	1.0	4	1	5e-4	300	512	512	512
Citeseer	0.4	0.4	1.0	1.0	0.8	4	2	5e-5	500	512	512	512
Pubmed	0.1	0.4	0.3	0.2	0.6	4	2	5e-4	1,000	512	512	512
Cora-A	0.3	0.2	0.6	0.5	0.6	0.5	0.5	1e-4	800	512	512	512
DBLP	0.2	0.2	0.8	0.2	1.0	0.0625	0.25	5e-3	500	256	256	256

## D Hypergraph Augmentations

Generating augmented views is crucial for contrastive learning methods. Different views provide different contexts or semantics for datasets. While creating semantically meaningful augmentations is crucial for contrastive learning, in the hypergraph domain, it is an underexplored problem than in other domains such as vision. In the (ordinary) graph domain, simple and effective graph augmentation methods have been proposed, and these are commonly used in graph contrastive learning [You et al., 2020, Zhu et al., 2020]. Borrowing these approaches, in this section, we analyze four types of augmentation (i.e., node masking, hyperedge masking, membership masking, and node feature masking), which are naturally applicable to hypergraphs, along with TriCon.

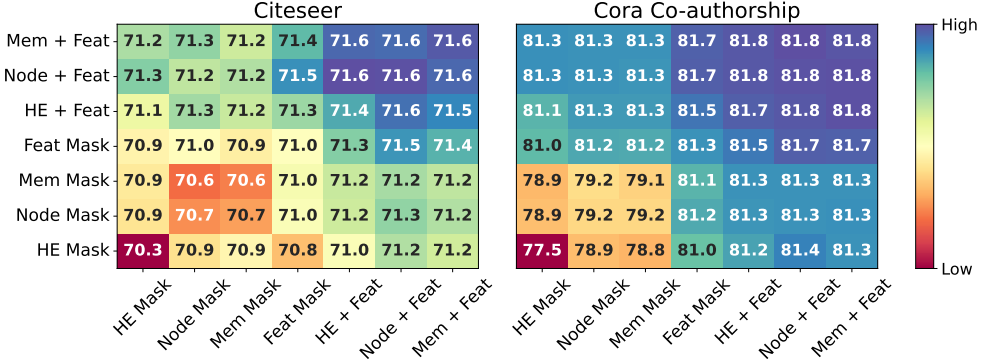


Figure 2: Node classification accuracy (%) when employing different augmentation pairs. Using the structural and attribute augmentations together always yields better performance than using just one.

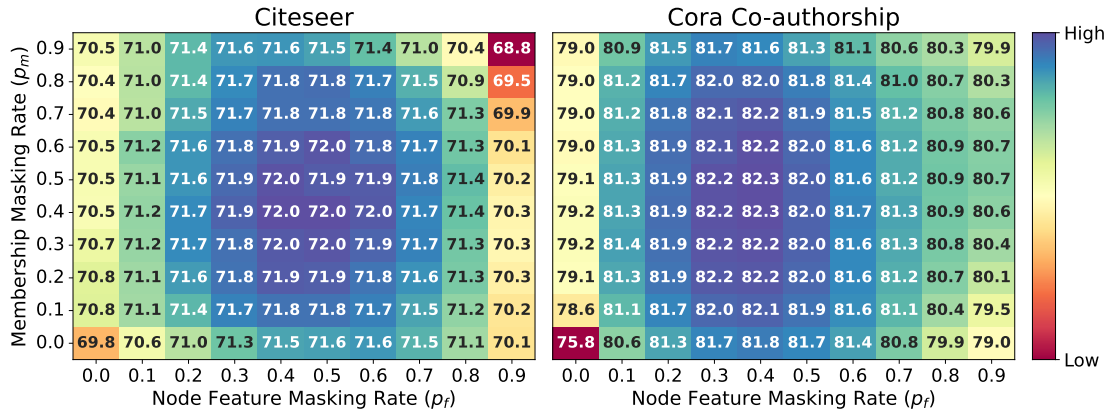


Figure 3: Node classification accuracy (%) according to the masking rates of membership and node features. A moderate extent of augmentation (i.e., masking rate between 0.3 and 0.7) benefits the downstream performance most.

- **Node masking:** randomly mask a portion of nodes in the original hypergraph. Formally, we use a binary mask of size  $|V|$  where each element is sampled from a Bernoulli distribution  $\mathcal{B}(1 - p_n)$  to mask nodes.
- **Hyperedge masking:** randomly mask a portion of hyperedges in the original hypergraph. Precisely, we use a binary mask of size  $|E|$  where each element is sampled from a Bernoulli distribution  $\mathcal{B}(1 - p_e)$  to mask hyperedges.
- **Membership masking:** randomly mask a portion of node-hyperedge memberships in the original hypergraph. In particular, we use a binary mask of size  $K = nnz(\mathbf{H})$  where each element is sampled from a Bernoulli distribution  $\mathcal{B}(1 - p_m)$  to mask node-hyperedge memberships.
- **Node feature masking:** randomly mask a portion of dimensions with zeros in node features. Specifically, we generate a single random binary mask of size  $F$  where each entry is sampled from a Bernoulli distribution  $\mathcal{B}(1 - p_f)$ , and use it to mask features of all nodes in the hypergraph.

The degree of augmentation can be controlled by  $p_n$ ,  $p_e$ ,  $p_m$ , and  $p_f$ . These masking methods corrupt the hypergraph structure, except for node feature masking, which impairs the hypergraph attributes.

To show which types of augmentation are advantageous, we first examine the node classification performance for different augmentation pairs with a masking rate of 0.2. We summarize the results in Figure 2. Note that, when using only one augmentation for each view, the effect of node feature masking is consistently good, but in particular, hyperedge masking performs poorly. Next, using the structural and attribute augmentations together always yields better performance than using just one. Among them, the pair of membership masking and node feature masking shows the best performance, demonstrating that using it in TriCon is a reasonable choice. The combination of node masking and node feature masking is also a good choice.

Figure 3 shows the node classification accuracy according to the membership and the node feature masking rate. It demonstrates that a moderate extent of augmentation (i.e., masking rate between 0.3 and 0.7) benefits the downstream performance most. If the masking rate is too small, two similar views are generated, which are insufficient to learn the discriminant ability of the encoder, and if it is too large, the underlying semantic of the original hypergraph is broken.

## E Additional Experiments

### E.1 Effects of Self-loops

In TriCon, we add self-loops to the hypergraph after hypergraph augmentation and before it is passed through the encoder. We conduct an ablation study to demonstrate the effects of self-loops. The results are summarized in Table 8, and it empirically verifies that adding self-loops is advantageous. The reason for the better performance we speculate is that a self-loop helps each node make a better use of its initial features. Specifically, a hyperedge corresponding to a self-loop receives a message only from the node it contains and sends a message back to the node without aggregating the features of any other nodes. This allows each node to make a better use of its features.

Table 8: Node classification accuracy (%) of TriCon when the hypergraphs, which the encoder receives as input, are with and without self-loops. Adding self-loops helps to improve the quality of the node representations. Cora-C and Cora-A stand for Cora Co-citation and Cora Co-authorship, respectively.

Dataset	TriCon	
	Without Self-loops	With Self-loops (Proposed)
Cora-C	$80.95 \pm 1.29$	<b><math>81.57 \pm 1.12</math></b>
Citeseer	$71.10 \pm 1.09$	<b><math>72.02 \pm 1.16</math></b>
Pubmed	$84.02 \pm 0.56$	<b><math>84.26 \pm 0.62</math></b>
Cora-A	$79.77 \pm 0.95$	<b><math>82.15 \pm 0.89</math></b>
DBLP	$90.19 \pm 0.12$	<b><math>91.12 \pm 0.11</math></b>

### E.2 Sensitivity Analysis

We investigate the impact of hyperparameters used in TriCon, especially,  $\tau_g$  and  $\tau_m$  in Eq. (8) and (10) as well as  $\omega_g$  and  $\omega_m$  in Eq. (11), with the Citeseer and Cora Co-citation datasets. We only change these hyperparameters in this analysis, and the others are fixed as provided in Appendix C.2.

We conduct node classification while varying the values of  $\tau_g$  and  $\tau_m$  from 0.1 to 1.0 and report the accuracy gain over TriCon-N, which only considers node-level contrast, in Figure 4. From the figure, it can be observed that TriCon achieves an accuracy gain in most cases when both the temperature parameters are not too small (i.e., 0.1), as shown in the blue area in the figure. It indicates that pursuing excessive uniformity in the embedding space rather degrades the node classification performance [Wang and Liu, 2021]. We also conduct the same task while varying the values of  $\omega_g$  and  $\omega_m$  from  $2^{-4}$  to  $2^4$  and report the accuracy gain over TriCon-N, in Figure 5. Using a large  $\omega_m$  and a small  $\omega_g$  together degrades the performance. This causes model collapse by making the proportion of membership-level contrastive loss relatively larger than node- and group-level contrastive losses.

## F Qualitative Analysis

As additional experiments, in Table 9, We provide t-SNE [Van der Maaten and Hinton, 2008] plots of the node representations produced by TriCon and its two variants, TriCon-N and TriCon-NG, on the Pubmed, Cora Co-authorship, and DBLP datasets. As expected from the quantitative results, the 2-D projection of embeddings learned by TriCon shows more numerically (based on Silhouette score [Rousseeuw, 1987]) distinguishable clusters than its two variants.

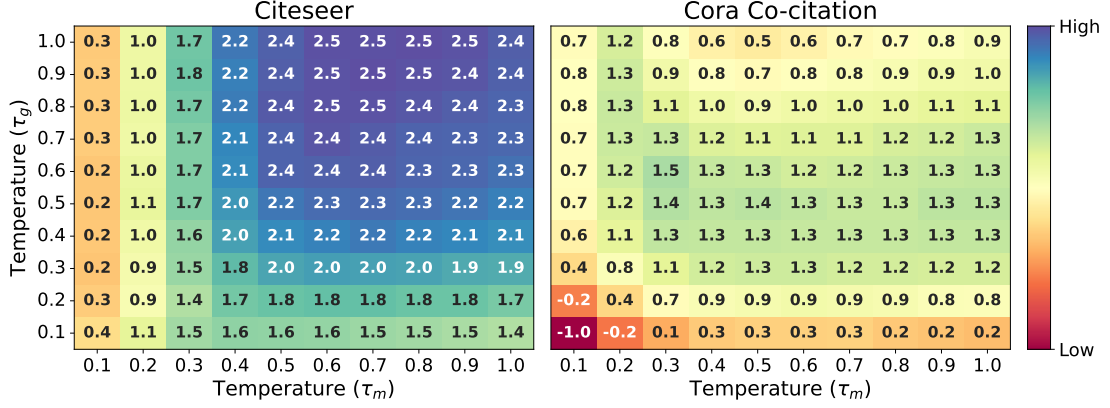


Figure 4: Node classification accuracy gain (%) of TriCon over TriCon-N, when different temperature parameter pairs are used. The baseline accuracies are 70.28% and 80.49% for the Citeseer and Cora Co-citation datasets, respectively.

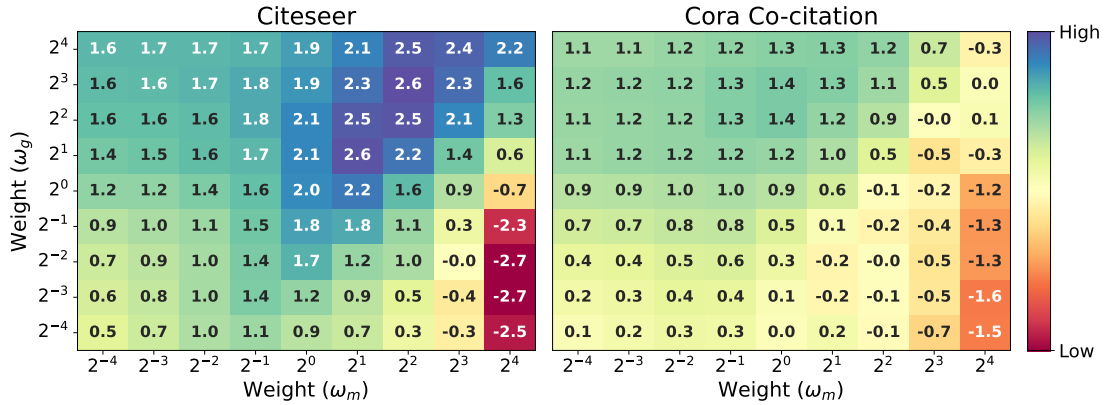


Figure 5: Node classification accuracy gain (%) of TriCon over TriCon-N, when different weight pairs are used. The baseline accuracies are 70.28% and 80.49% for the Citeseer and Cora Co-citation datasets, respectively.

Table 9: t-SNE plots of the node representations from TriCon and its two variants. The TriCon's embeddings exhibits the most distinct clusters with the help of group and membership contrast, as measured by the Silhouette score (the higher, the better).

